Modeling the Compression Set of Elastomers to Predict the Lifetime of Sealing Systems by Finite Element Analysis

Dr.-Ing. Christoph Wehmann, Ambarish Kulkarni, B.Eng., Feyzan Durn, M.Sc., Dr. Murat Gulcur

In many cases, the lifetime of a sealing system is limited by the compression set of the elastomer. Therefore, it would be beneficial to have a numerical procedure which can capture the compression set. This contribution starts with an overview of the existing literature in this field. Next, a method based on previous research work is developed and described. It allows to predict both the decrease of the sealing force and the resulting permanent deformation. This prediction can be done for long time scales. The results of this method are compared to experimental values of a fluorine-based elastomer. Finally, the aging of an O-ring is simulated by the developed method.

1 Introduction

The lifetime of sealing systems relies on various parameters, depending on the material and the application. In case of thermoset elastomer seals, the sealing function and lifetime often is limited by the permanent deformation of the sealing material under compression which is called compression set [1]. Upon the lifetime of the sealing material the cross-linking chemical bonds holding the polymer chains together can break down or can rearrange at different positions. This leads to plastic strains which are not driven by the stress level as it would be in classical rate-independent plasticity. It is a time-driven chemical reaction with a given rate and accordingly, the unloaded shape of the seal will continuously change.

The permanent deformation of the seal also causes a decrease of the stresses and hence, a decrease of the corresponding sealing force. An appropriate simulation method can predict the permanent deformation and stress relaxation to estimate the lifetime of the sealing system. It requires a material model which is capable to describe the compression set and the corresponding stress relaxation.

Chapter 2 contains a description of aging effects in elastomers and their microstructural explanation. Furthermore, it contains a literature overview over research work in the area of compression set modeling in general and in sealing technology applications. In chapter 3, a method based on previous research work is developed and described. The method can be used to carry out lifetime predictions of sealing systems.

In chapter 4, the prediction of the model is applied to a fluorine-based elastomer and compared to experimental results. Finally, the method is applied to an O-ring and the results are discussed in chapter 5.

2 State of the Art

In order to model the compression set, the basic understanding of aging is crucial. Therefore, the knowledge about its explanation on a molecular level is described first. In subchapter 2.2, the scientific work around modelling the compression set in FEA is reported.

2.1 Aging Effects in Elastomers and their Microstructural Explanation

Elastomeric seals can be exposed to cyclic or continuous media during their service life. As a result, their mechanical performance is degraded over time which is commonly known as aging. Exposure to air, water, exposure to UV light or ozone, thermal oxidation, or chemically reactive environments can all cause aging, see e.g. Bahroloumi [2]. Unless used in vacuum or chemically inert environments, almost all polymers are susceptible to oxidation. Oxidation is a thermally driven degradation which occurs at slow rates at ambient temperatures. Thus, to accelerate oxidation and predict the lifetime of seals, aging tests are performed at elevated temperatures [3].

In an elastomer formulation, there are mainly 4 ingredients: base cross-linkable polymer, curing agents, fillers and stabilizers. The viscoelastic properties of an elastomeric material are inherent from the polymer which is the primary ingredient of the formulation. The polymer chains are cross-linked to maintain the shape and viscoelasticity of the moulded parts [4]. During the aging process, any of these ingredients can be affected. However, the changes of the primary base polymer will affect the material properties the most.

When the temperature is increased to elevated levels, the primary valance bonds in polymers can start to break which leads to chain scission. If scission occurs between the main chain and the side groups, double bonds and crosslinks may start to form. In this case, polymers stabilize upon heating and a relaxation of stresses with time occurs due to the chemical reactions [5, 6]. In the high temperature regime, elastomers can either soften or harden, either of which eventually leads to a loss in their desirable properties. Depending on the aging type and mechanism, the cross-links between the polymer chains can break. In that case the material will soften. If the polymer chains start to bind upon heating, the material hardens due to excessive cross-linking. Hardened elastomers will become more susceptible to forming cracks under stresses [7]. Exposure to the external media can also cause chain-scission or breakage of intermolecular cross-links leading to a loss in material properties.

Finally, under compressive stresses aging effects will be more severe which was investigated by Li et al. [8]. They tested loaded and unloaded EPDM gaskets and observed this negative effect of compressive stresses on the aging behaviour.

2.2 Modelling the Compression Set in Finite Element Analysis

During aging bonds within the 3-dimensional network are relocating in a stress-free configuration. This leads to a decrease of the stresses and to a permanent deformation which increases over time. Achenbach considers this relocation procedure to develop a model which is able to capture the corresponding aging effects and the

compression set [9, 10]. He starts from the Neo-Hookean hyperelastic model which can be formulated by using the number of cross-links N in the rubber network:

$$\sigma = 2\,C_{10}\,(\lambda - \lambda^{-2}) = 2\,N\,c\,(\lambda - \lambda^{-2}) \tag{1}$$

In this equation, σ is the Cauchy stress, C_{10} is the Neo-Hooke material parameter, λ is the principal stretch, N is the number of cross-links in the rubber and c is another material parameter. While c is constant, $N = N(t)$ is already modeling the stress decrease when bonds are broken.

Equation (1) is the 1-dimensional representation of the Neo-Hookean law and the corresponding principal stretch in a tensile test is given by equation (2) where l is the deformed length and l_0 is the undeformed length of the tensile specimen.

$$\lambda = \frac{l}{l_0} \tag{2}$$

The Neo-Hookean material parameter C_{10} is directly connected to the shear modulus of the material [11], see equation below.

$$G = 2\,C_{10} \tag{3}$$

Next, Achenbach introduces the stress contribution by the relocated bonds – he is defining a “second” network of bonds where the number of curing bonds is given by M. Furthermore, this second network has a different undeformed configuration which is the current deformed state. This new undeformed configuration is described by the principal stretch $\hat{\lambda}$. Finally, Achenbach formulates the equation below for the total Cauchy stress resulting from both the original and the new network.

$$\sigma = 2\,N\,c\,(\lambda - \lambda^{-2}) + 2\,M\,c\left(\lambda\,\hat{\lambda}^{-1} - \lambda^{-2}\,\hat{\lambda}^{2}\right) \tag{4}$$

Here, the total number of bonds is assumed to be constant.

$$N_0 = N(t) + M(t) \tag{5}$$

For the change of N over time, Achenbach proposes an exponential law:

$$N(t) = N_0\,e^{-\frac{t}{\tau}} \tag{6}$$

From equation (5) and (6), the formula for $M(t)$ can be derived too. Finally, Achenbach transfers this approach to a 3-dimensional stress state and formulates the stress equation as shown below [10].

$$\sigma_{ij} = -p\,\delta_{ij} + 2\,\frac{\partial W_0}{\partial \bar{I}_1}\,B_{ij} + 2\int_{\tau=0}^{t} \frac{d}{d\tau}\left(\frac{\partial \widehat{W}}{\partial \hat{I}_1}\right)\hat{B}_{ij}\,d\tau \tag{7}$$

Here, p is the hydrostatic pressure, B_{ij} are the coordinates of the left Cauchy-Green tensor, W_0 is the hyperelastic strain energy density function of the old network and $\widehat{W}$ is the strain energy density function of the “second” network which can change continuously. This approach assumes a split of the strain energy density function into an isochoric and a volumetric part [12]. The material is considered to be incompressible and therefore, only the isochoric part remains which is described by W_0

respectively $\widehat{W}$. Accordingly, the strain energy function W_0 is a function of the first invariant of the isochoric part of the right Cauchy-Green tensor which is symbolized by $\bar{I}_1$ while I_1 would be the first invariant of the complete Cauchy-Green tensor. For the second network, only one symbol will be introduced which describes the first invariant of the isochoric part of the right Cauchy-Green tensor: $\hat{I}_1$. This is describing the deformation of the second or new network and this has a different undeformed configuration which can change over time.

Accordingly, the isochoric strain energy density function of Achenbach's model is:

$$\begin{aligned} W &= \underbrace{\widetilde{N}\, C_{10}(\bar{I}_1 - 3)}_{W_0} + \int_{\tau=0}^{t} \frac{d\widehat{W}}{d\tau}\, d\tau \\ &= \widetilde{N}\, C_{10}(\bar{I}_1 - 3) + \int_{\tau=0}^{t} \frac{d\widetilde{M}}{d\tau} C_{10}\left(\hat{I}_1 - 3\right) d\tau \end{aligned} \tag{8}$$

Here, $\widetilde{N}$ and $\widetilde{M}$ are the unified numbers of bonds according to the equation below.

$$\begin{aligned} \widetilde{N} &= N/N_0 \\ \widetilde{M} &= M/M_0 \end{aligned} \tag{9}$$

The left summand in equation (8) belongs to the well-known Neo-Hookean strain energy density function if $\widetilde{N} = 1$, see e.g. [13]. The left summand in equation (8) is decreasing over time which describes the break down of the primary network of bonds. The right summand (the integral) is describing the build up of the new network (secondary network).

Lion and Johlitz also develop a model to describe the compression set in elastomers and they use a time-dependent approach which is similar to the one Achenbach proposed [14]. They also assume that the old or primary network of bonds is breaking down continuously while a new network (secondary network) is building up in the deformed state. Accordingly, they formulate a split strain energy density function as shown in equation (8). In addition, they consider a volumetric deformation and the corresponding strain energy density function and introduce a similar time dependence to the volumetric response. This allows them to capture volume changes due to aging effects. They derive all equations of the required continuum mechanics in detail.

Johlitz is continuing this work and proposes two new material models to capture aging effects in elastomers [15]. The first model is based on a split of the isochoric strain energy density function into two parts: one referring to the old (primary) network of bonds and one referring to the new (secondary) network of bonds. This approach is similar to the approaches described above. However, while Achenbach is formulating this on the basis of the Neo-Hookean law of hyperelasticity, Johlitz is using a Mooney type of strain energy density. Johlitz also shows that for the case of constant temperatures his model describes the number of network bonds by the same exponential law as proposed by Achenbach (see equation (6)).

The second model Johlitz introduces couples diffusion and aging effects [15]. It allows to model aging effects depending on the concentration of oxygen inside the elastomer. This dependence can be inhomogeneous and requires the solution of the concentration field in addition to the displacement field. For both models, Johlitz derives all continuum equations for the three-dimensional case and implements them into the finite element code PANDAS.

Bahrololoumi et al. develop a model to describe aging effects which is based on a decay function integration into the strain energy density function [2]. Bahrololoumi et al. derive the stress-strain relationships by using the second Piola-Kirchhoff stress tensor and they are able to capture the decay of mechanical properties in a 3D stress state. The aging effects are modelled by referring to the undeformed configuration. They also derive the material tangent tensor and implement their model into an FEA code by using the Total Lagrangian element formulation. Details to the Total Lagrangian formulation and its implementation into the FEA code Z88 are described by Rieg et al. [16].

Maiti et al. are modeling the compression set of a silicone elastomer which is caused by radiation [17]. They use the model of Tobolsky to formulate a one-dimensional relationship between the permanent set, the radiation dose and the strain at which the radiation-induced aging takes place. Their model allows to predict the stress-strain behavior, the permanent set and the crosslink density of the rubber.

3 Method to Model the Compression Set in Finite Element Analysis

In the previous chapter several methods to capture compression set are listed and described. The model of Achenbach was already successfully applied to sealing systems and it is able to capture both compression set and compressive stress relaxation. Furthermore, it can be combined with time-temperature-shifting which allows to use short time tests to calibrate a long-term material model. Therefore, the model of Achenbach will be used in the following.

The material model will be implemented by using a split of the deformation into an isochoric and a volumetric part. Accordingly, deformation gradient $\boldsymbol{F}$, the right Cauchy-Green tensor $\boldsymbol{C}$ and the left Cauchy-Green tensor $\boldsymbol{B}$ are split as shown below [12].

$$\boldsymbol{F} = \boldsymbol{F}_v\,\overline{\boldsymbol{F}} = J^{\frac{1}{3}}\,\mathbf{1}\;\; J^{-\frac{1}{3}}\boldsymbol{F} \tag{10}$$

$$\overline{\boldsymbol{C}} = J^{-\frac{2}{3}}\,\boldsymbol{C} \tag{11}$$

$$\boldsymbol{B}_v = J^{\frac{2}{3}}\,\mathbf{1}; \qquad \overline{\boldsymbol{B}} = J^{-\frac{2}{3}}\,\boldsymbol{B} \tag{12}$$

For each quantity, the volumetric part is symbolized by the index v and the isochoric part is symbolized by the accent $\overline{\;}$, for example $\overline{\boldsymbol{B}}$. It will be assumed that the material behaves incompressible, hence the volumetric part of the deformation vanishes and $J = 1$ holds. Nevertheless, the determinant J will be left a variable towards the end of this chapter.

In order to use the Achenbach model within FEA, a user subroutine has to be implemented. The user subroutine will be developed to be used by the FEA code Abaqus. It was chosen to use a user subroutine of the type UMAT (user material subroutine) which provides the highest level of freedom to model extensions of the constitutive law. Furthermore, it leads to the fastest convergence when implemented efficiently.

In the following, the strain energy density function of Achenbach's model (8) will be used. The Cauchy stress tensor can be split into three parts: a hydrostatic part, a deviatoric part $\boldsymbol{s}$ belonging to the primary elastomer network and a deviatoric $\hat{\boldsymbol{s}}$ part belonging to the new, secondary elastomer network.

$$\boldsymbol{\sigma} = -p\,\mathbf{1} + \boldsymbol{s} + \hat{\boldsymbol{s}} \tag{13}$$

The derivation with respect to the right Cauchy-Green tensor $\boldsymbol{C}$, pushed forward to the current deformation state leads to the Cauchy stress tensor [18]. Equation (14) shows this operation for the deviatoric part of the primary network.

$$\boldsymbol{s} = \frac{1}{J}\,\boldsymbol{F}\,\overline{\boldsymbol{S}}\,\boldsymbol{F}^T = \frac{2}{J}\,\boldsymbol{F}\,\frac{\partial W_0}{\partial \boldsymbol{C}}\,\boldsymbol{F}^T \tag{14}$$

Here, $\overline{\boldsymbol{S}}$ is the deviatoric part of the second Piola-Kirchhoff stress tensor. Since the strain energy density function of the primary network W_0 is formulated as a function of the first invariant of the isochoric part of right Cauchy-Green tensor, the chain rule can be used to calculate the derivatives. Wriggers derives the chain rule for this case as shown below [18].

$$\frac{\partial W_0}{\partial C_{ij}} = \frac{\partial W_0}{\partial \bar{C}_{kl}}\,\frac{\partial \bar{C}_{kl}}{\partial C_{ij}} \tag{15}$$

$$\frac{\partial \overline{\boldsymbol{C}}}{\partial \boldsymbol{C}} = J^{-\frac{2}{3}}\left(\mathbb{E} - \frac{1}{3}\,\boldsymbol{C}^{-1} \otimes \boldsymbol{C}\right) \tag{16}$$

The index notation of equation (16) is shown below.

$$\frac{\partial \bar{C}_{ij}}{\partial C_{kl}} = J^{-\frac{2}{3}}\left(\mathbb{E}_{ijkl} - \frac{1}{3}\,C_{ij}\,C^{-1}_{kl}\right) \tag{17}$$

In equation (16), $\mathbb{E}$ is a fourth order unit tensor defined as:

$$\mathbb{E}_{ijkl} = \frac{1}{2}\left(\delta_{ik}\delta_{jl} + \delta_{il}\delta_{jk}\right) \tag{18}$$

Inserting (15)-(18) into (14) leads to the following result for the deviatoric stresses.

$$s_{ij} = \frac{2}{J}\,F_{ik}\,F_{jl}\,\widetilde{N}\,C_{10}\,\delta_{mn}\,J^{-2/3}\left\{\mathbb{E}_{mnkl} - \frac{1}{3}\,C_{mn}\,C^{-1}_{kl}\right\} \tag{19}$$

After some transformations this form can be derived:

$$s_{ij} = \frac{2}{J}\;\widetilde{N}\,C_{10}\left\{J^{-2/3}\,\underbrace{\frac{1}{2}\left(F_{im}\,F_{jm} + F_{im}\,F_{jm}\right)}_{=B_{ij}} - \frac{1}{3}\,\underbrace{J^{-2/3}\,C_{mm}}_{\bar{C}_{mm}}\,\delta_{ij}\right\} \tag{20}$$

It can be seen that only the isochoric parts of the deformation tensor will be remaining. Since $\bar{C}_{mm} = \bar{B}_{mm}$ holds, the deviatoric stresses from the primary network finally becomes:

$$\boldsymbol{s} = \frac{2}{J}\ \widetilde{N}\ C_{10}\ \left\{\overline{\boldsymbol{B}} - \frac{1}{3}\ tr(\overline{\boldsymbol{B}})\ \mathbf{1}\right\} \tag{21}$$

Very similar the deviatoric stresses of the newly formed, secondary elastomer network can be derived. However, in the secondary network the stress-free configuration is different. It is the configuration in which this network established and this can be different for each "single" bond which re-bonded. Therefore, a new deformation gradient $\widehat{\boldsymbol{F}}$ is introduced which describes the deformation between the configuration in which the aging took place and the current configuration. Since the aging can take place at different times with different configurations, this deformation gradient is a function of time $\widehat{\boldsymbol{F}} = \widehat{\boldsymbol{F}}(t)$. This time dependence also occurs in quasi-static loading conditions where during aging the deformation is continuously changing. Figure 1 displays the definition of this additional deformation gradient.

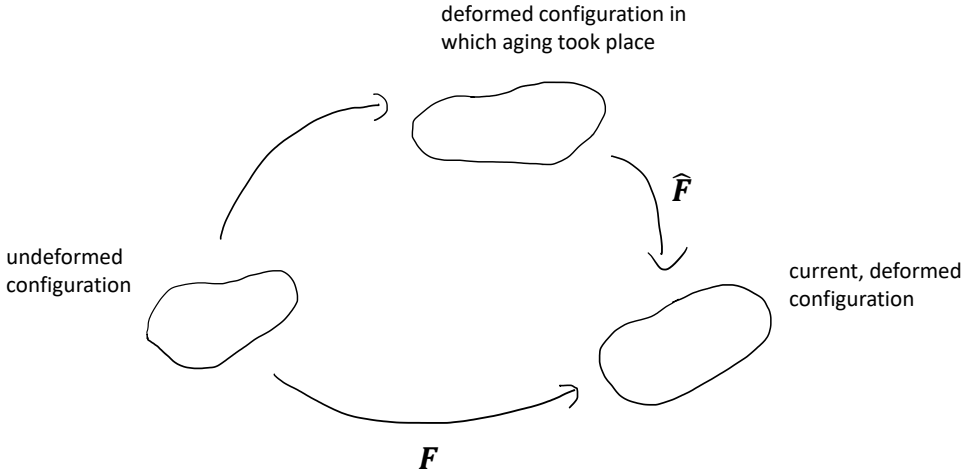

Figure 1: Definition of the deformation gradients

Accordingly, the stresses of the secondary network can be derived as follows.

$$\hat{\boldsymbol{s}} = \frac{1}{\hat{J}}\ \boldsymbol{F}\ \widehat{\overline{\boldsymbol{S}}}\ \boldsymbol{F}^T = \frac{2}{\hat{J}}\ \widehat{\boldsymbol{F}}\ \frac{\partial \widehat{W}}{\partial \widehat{\boldsymbol{C}}}\ \widehat{\boldsymbol{F}}^T; \qquad \widehat{\boldsymbol{C}} = \widehat{\boldsymbol{F}}^T\ \widehat{\boldsymbol{F}} \tag{22}$$

By the same steps as for the primary network, the final expression for the deviatoric stresses of the secondary network can be obtained.

$$\hat{\boldsymbol{s}} = C_{10} \int_{\tau=0}^{t} \frac{2}{\hat{J}}\ \frac{d\widetilde{M}}{d\tau} \left\{\widehat{\overline{\boldsymbol{B}}} - \frac{1}{3}\ tr(\widehat{\overline{\boldsymbol{B}}})\ \mathbf{1}\right\} d\tau \tag{23}$$

Equation (24) defines the total Cauchy stress tensor.

$$\boldsymbol{\sigma} = -p\ \mathbf{1} + \frac{2}{J}\ \widetilde{N}\ C_{10}\ \left\{\overline{\boldsymbol{B}} - \frac{1}{3}\ tr(\overline{\boldsymbol{B}})\ \mathbf{1}\right\} + C_{10} \int_{\tau=0}^{t} \frac{2}{\hat{J}}\ \frac{d\widetilde{M}}{d\tau} \left\{\widehat{\overline{\boldsymbol{B}}} - \frac{1}{3}\ tr(\widehat{\overline{\boldsymbol{B}}})\ \mathbf{1}\right\} d\tau \tag{24}$$

For the development of the code implementation, the 4th order material tensor $\mathbb{C}$ has to be derived according to the equation shown below [19]. This equation results from

the choice of the Jaumann stress rate to calculate an objective time derivative of the stress tensor [18].

$$\delta\boldsymbol{\tau} - \delta\boldsymbol{W}\,\boldsymbol{\tau} + \boldsymbol{\tau}\,\delta\boldsymbol{W} = J\,\mathbb{C} : \delta\boldsymbol{D} \tag{25}$$

In this equation, $\boldsymbol{\tau} = J\,\boldsymbol{\sigma}$ is the Kirchhoff stress tensor, $\boldsymbol{W}$ is the spin tensor and $\boldsymbol{D}$ is the rate of deformation tensor. Since Abaqus uses an Updated Lagrangian element formulation, the material tensor needs to be derived by considering the virtual rate of deformation $\delta\boldsymbol{D}$ [20]. The symbol δ in equation (25) is used for virtual quantities. Through the equations (8), (24) and (25) the material model is completely defined.

4 Comparison of the Model Prediction to Experimental Data

In the following, experimental data of a fluorine-based elastomer used in sealing applications is considered and compared to simulation results. The compression set was tested for several different time durations from 24 hours to 1008 hours. These tests were carried out at different temperatures and then shifted to ambient temperature. The shifting is based on the time-temperature equivalence. Figure 2 shows the resulting master curve which is valid at ambient temperature. The diagram contains values up to 300,000 hours (approx. 34 years). Furthermore, the model prediction of the Achenbach model is shown. From equation (6), the formula of the compression set can be obtained:

$$c_s(t) = \left(1 - e^{-\frac{t}{\tau}}\right) \cdot 100\ \% \tag{26}$$

The curve shown in figure 2 is based on an aging parameter of $\tau = 3800\ days$.

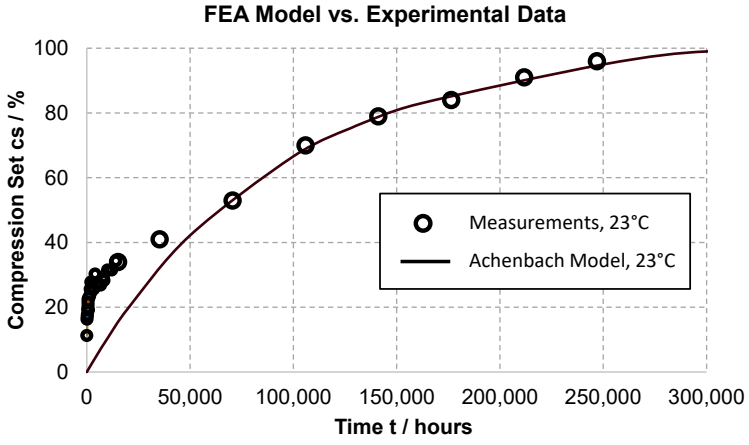

Figure 2: Model prediction and experimental data of compression set at 23°C

It can be seen that the Achenbach model predicts the behavior of the material very well from medium to long time durations. For short time durations up to 50,000 hours (= approx. 6 years), the model predicts lower values for the compression set. However, since the simulation method will be used for lifetime predicitons, the short time scales are not relevant. For the purpose of lifetime predictions, the Achenbach model

shown in Figure 2 is suited very well. And it is remarkable that the model predicts the aging behavior very well by only using one single material parameter.

5 Application of the Method to Analyse the Lifetime of an O-ring

In the following an O-ring sealing system will be considered. The cross section diameter of the O-ring is 5 mm. To reduce the computational effort, only a section of the complete O-ring will be modelled as displayed in Figure 3. The O-ring is sealing a vacuum chamber and accordingly, a pressure of 1 bar is applied on the left in figure 3. The material parameters of the fluorine-based elastomer are listed in Table 1, compare also chapter 4.

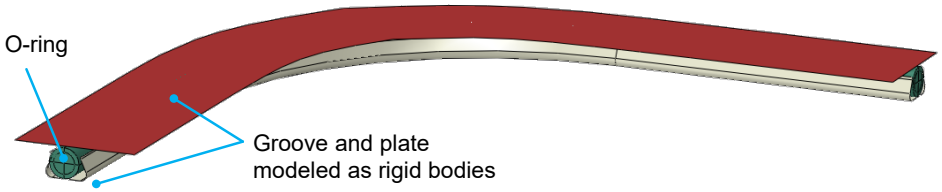

Figure 3: Model of the O-ring and the surrounding hardware

Table 1: Parameters of the material model, valid at 23°C

	Symbol	**Value** (d = days)
Neo-Hooke parameter	C_{10}	$1.29\ N/mm^2$
Achenbach parameter	τ	$3800\ d$

Two simulations with different aging times are considered in the following. The first simulation is divided in three steps and considers a time duration of 15 years:

1) Assembly of the O-ring
2) Aging for 15 years
3) Disassembly of the O-ring

After the disassembly, the permanent deformation due to the compression set can be displayed. Figure 4 shows these results, the colour describes the displacement. This result allows to determine the remaining height of the unloaded O-ring which is 4.25 mm after 15 years. Hence, it is reduced by 0.75 mm. Since the groove height is 4 mm, 0.25 mm of the O-ring are remaining for the elastic deformation which generates the sealing force.

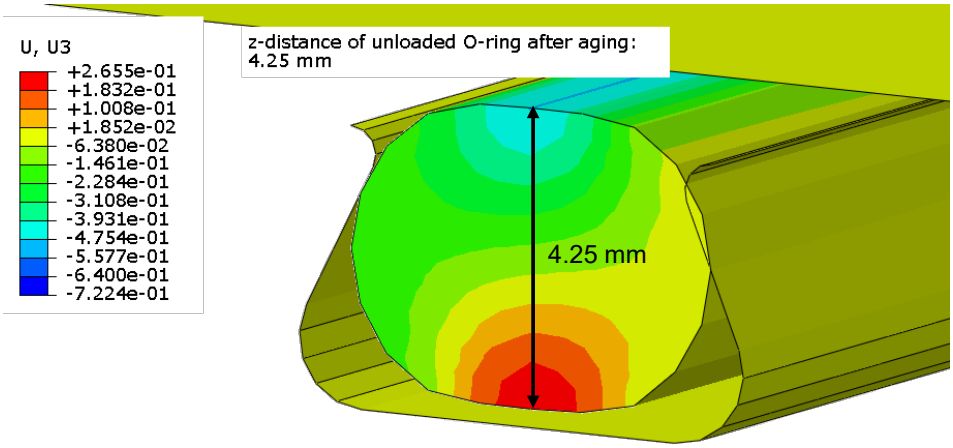

Figure 4: Resulting permanent displacement after 15 years of aging

The second simulation is also divided in three steps and considers a time duration of 37 years:

1) Assembly of the O-ring
2) Aging for 37 years
3) Disassembly of the O-ring

The diagram below displays the decrease of the sealing force over time. It can be seen that it reaches 0 N/cm after 37 years. This is due to the fact that the compression set reaches 100 % after 37 years at 23°C.

For the application in which this O-ring is operating, it is known from experience that the sealing force should be min. 1 N/cm to guarantee the sealing function. Hence, from the FEA results it can be derived that the lifetime of the sealing system is approximately 32 years.

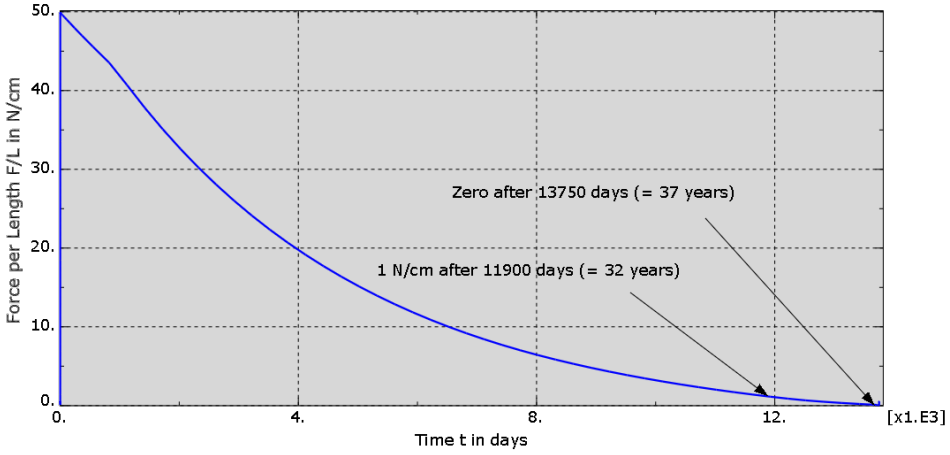

Figure 5: Decrease of the sealing force over time

6 Summary, Conclusion and Outlook

The present contribution describes the effects which are happening during aging of elastomers and provides their microstructural explanation as far as known today. Next, an overview over research work dealing with modelling the compression set is given. The model of Achenbach is used to develop a numerical method which allows to capture the compression set within an FEA. This method is implemented into an Abaqus user subroutine (UMAT). Finally, the method is applied to an O-ring which seals a vacuum chamber and the resulting permanent deformation after long time duration is predicted. Furthermore, the decrease of the sealing force over 37 years is calculated.

The prediction of the Achenbach model for an fluorine-based elastomer compares well against experimental data when medium or long time scales are considered. The FEA based method works well to analyse the permanent deformation (set) of fluorine-based elastomers after years of aging. Furthermore, it allows to predict the decrease of the sealing force.

Future work could consider more complex mathematical functions with more parameters to model the aging effects. This might allow to have an improved fitting accuracy over the whole time duration. Furthermore, the method could be extended to other hyperelastic laws or combined with viscoelasticity. Finally, the presented approach could be coupled with additional physical and chemical effects. For example, the material model could be coupled with the method of Plagge et al. which allows to capture the Mullins effect in a very accurate way [21]. This way the damage through cyclic loading and the compression set through aging could be included in FEA.

7 Acknowledgements

The authors would like to sincerely thank Dr. Manfred Achenbach for the very educative and helpful discussions about his publications dealing with modelling aging effects in elastomers. His pioneering and outstanding scientific work in this field was the basis for the present work.

8 Nomenclature

Variable	*Description*	*Unit*
$\boldsymbol{B}$	Left Cauchy-Green strain tensor	$[-]$
$\overline{\boldsymbol{B}}$	Isochoric part of the left Cauchy-Green strain tensor	$[-]$
$\boldsymbol{B}_v$	Volumetric part of the left Cauchy-Green tensor	
$\widehat{\overline{\boldsymbol{B}}}$	Isochoric part of the left Cauchy-Green strain tensor, where the reference configuration (stress-free configuration) is the deformation state in which the aging took place	$[-]$
$\boldsymbol{C}$	Right Cauchy-Green strain tensor	$[-]$
$\overline{\boldsymbol{C}}$	Isochoric part of the right Cauchy-Green strain tensor	$[-]$
$\widehat{\overline{\boldsymbol{C}}}$	Isochoric part of the Cauchy-Green strain tensor, where the reference configuration (stress-free configuration) is the deformation state in which the aging took place	$[-]$
$\mathbb{C}$	4th order material tensor	$[N/mm^2]$
C_{10}	Neo-Hooke material parameter	$[N/mm^2]$
δ_{ij}	Kronecker Symbol	N/mm^2
$\delta\boldsymbol{D}$	Variation of the rate of deformation tensor $\boldsymbol{D}$ (virtual rate of deformation)	$[1/sec]$
$\boldsymbol{F}$	Deformation gradient	$[-]$
$\overline{\boldsymbol{F}}$	Isochoric part of the deformation gradient	$[-]$
$\boldsymbol{F}_v$	Volumetric part of the deformation gradient	
$\widehat{\boldsymbol{F}}$	Deformation gradient, where the reference configuration (stress-free configuration) is the deformation state in which the aging took place	$[-]$
λ	Principal stretch in a one-dimensional stress state (tensile test), eigenvalue of the deformation gradient	$[-]$
$\boldsymbol{\sigma}$	Cauchy stress tensor, sum of primary and secondary network of the elastomer	$[N/mm^2]$
$\boldsymbol{s}$	Deviatoric part of the Cauchy stress tensor, resulting from the primary network	$[N/mm^2]$
$\hat{\boldsymbol{s}}$	Deviatoric part of the Cauchy stress tensor, resulting from the secondary (new) network	$[N/mm^2]$
$\boldsymbol{S}$	Second Piola-Kirchhoff stress tensor, sum of primary and secondary network of the elastomer	$[N/mm^2]$
$\overline{\boldsymbol{S}}$	Deviatoric part of the second Piola-Kirchhoff stress tensor	$[N/mm^2]$
τ	Material parameter in the Achenbach model	$[d]$

9 References

[1] Müller, H. K., Nau, B. S., *Fluid Sealing Technology. Principles and Applications,* Marcel Dekker, Inc., New York, Basel, Hong Kong, 1998.

[2] Bahrololoumi, A., Mohammadi, H., Moravati, V., Dargazany, R.: *A Physically-Based Model for Thermo-Oxidative and Hydrolytic Aging of Elastomers*. International Journal of Mechanical Sciences, vol. 194, ID 106193, pp. 1-13, 2021

[3] White, J. R.: Polymer Ageing: Physics, Chemistry or Engineering? Time to Reflect, Chimie, vol. 9, pp 1396-1408, 2006

[4] Arachchige, W.N.B.: *Aging and long-term performance of elastomers for utilization in harsh environments*. PhD thesis, Chair of Materials Science and Testing of Polymers, Montanuniversität Leoben, Austria, 2019

[5] Throdahl, M. C.: *Aging of Elastomers - Comparison of Creep with Some Conventional Aging Methods*. Industrial & Engineering Chemistry, vol. 40, pp. 2180-2184, 1948

[6] Madorsky, S. L., Straus, S.: Thermal Degradation of Polymer at High Temperatures. Journal of Research of the National Bureau of Standards, vol. 63A, no. 3, pp. 261-268, 1959

[7] Celina, M. C.: Review of polymer oxidation and its relationship with materials performance and lifetime prediction. Polymer Degradation and Stability, vol. 98, pp. 2419-2429, 2013

[8] Li, C., Ding, Y., Yang, Z., Yuan, Z., Ye, L.: *Compressive stress-thermo oxidative aging behaviour and mechanism of EPDM rubber gaskets for sealing resilience assessment*. Polymer Testing, vol. 84, ID 106366, 2020

[9] Achenbach, M.: *Service life of seals – numerical simulation in sealing technology enhances prognoses*. In: Computational Materials Science, vol. 19, pp. 213-222, 2000.

[10] Achenbach, M.: *Modellierung der Alterung von Gummi*. (English translation: *Modeling the Aging of Rubber*). In: P. Streit, M. Achenbach, R. Boschet, E. Hörl, P. Krumreich, R. Kuschel, F. Leibbrandt, R. Lenz, J. Reichert, U. Wallner: Elastomere Dichtungssysteme. Werkstoffe – Anwendungen – Konstruktionen – Normen. expert Verlag, Renningen, 2011

[11] Holzapfel, G.: *Nonlinear Solid Mechanics: A Continuum Approach for Enineering*. Wiley, 2000

[12] Parisch, H., *Festkörperkontinuumsmechanik. Von den Grundgleichungen zur Lösung mit Finiten Elementen,* Teubner, Stuttgart, 2003.

[13] Ogden, R. W., *Non-Linear Elastic Deformations*. Dover Publications, Inc., Mineola, New York, 1997.

[14] Lion, A., Johlitz, M.: *On the representation of chemical ageing of rubber in continuum mechanics*. International Journal of Solids and Structures, vol. 49, pp. 1227-1240, 2012

[15] Johlitz, M.: *Zum Alterungsverhalten von Polymeren: Experimentell gestützte, thermo-chemomechanische Modellbildung und numerische Simulation*. (English translation: *The Aging Behavior of Polymers: Thermo-chemo-mechanical modeling and numerical simulation including experimental verification*). Habilitation thesis, Universität der Bundeswehr München, Munich, 2015

[16] Rieg, F., Hackenschmidt, R., Alber-Laukant, B.: *Finite Element Analysis for Engineers. Basics and Practical Applications with Z88Aurora*. Carl Hanser, München, 2014

[17] Maiti, A., Gee, R.H., Weisgraber, T., Chinn, S., Maxwell, R.S.: *Constitutive Modeling of Radiation Effects on the Permanent Set in a Silicone Elastomer*. Polymer Degradation and Stability, vol. 93, pp. 2226-2229, 2008

[18] Wriggers, P.: Nonlinear Finite Element Methods. Springer, Berlin, Heidelberg, 2010

[19] Dassault Systemes Simulia: Abaqus Training Class “Writing User Subroutines with Abaqus”. Training class script, 2013

[20] Bathe, K.-J., Ramm, E., Wilson, E. L.: *Finite Element Formulations for Large Displacement Dynamic Analysis*. International Journal for Numerical Methods in Engineering, vol. 9, pp. 353-386, 1975

[21] Plagge, J., Ricker, A., Kröger, N.H., Wriggers, P., Klüppel, M.: Efficient Modeling of Filled Rubber Assuming Stress-Induced Microscopic Restructurization. International Journal of Engineering Science, vol. 151, pp. 1-20, 2020

10 Authors

Trelleborg Sealing Solutions Germany GmbH

Schockenriedstr. 1, 70565 Stuttgart, Germany:

Dr.-Ing. Christoph Wehmann, christoph.wehmann@trelleborg.com

Ambarish Kulkarni, B.Eng., ambarish.kulkarni@trelleborg.com

Trelleborg Sealing Solutions UK Ltd.

Tewkesbury Business Park, International Drive, Tewkesbury, GL20 8UQ, UK

Feyzan Durn, M.Sc., feyzan.durn@trelleborg.com

Dr. Murat Gulcur, murat.gulcur@trelleborg.com